ELSEVIER

Biophysical Chemistry 71 (1998) 185–198

Biophysical Chemistry

On the need to consider kinetic as well as thermodynamic consequences of the parking problem in quantitative studies of nonspecific binding between proteins and linear polymer chains

Peter D. Munro [a,1], Craig M. Jackson [b], Donald J. Winzor [a,*]

[a] *Centre for Protein Structure, Function and Engineering, Department of Biochemistry, University of Queensland, Brisbane, Queensland 4072, Australia*

[b] *5931 Seacrest View Road, San Diego, CA 92121-4352, USA*

Received 26 December 1997; accepted 29 December 1997

Abstract

Attention is drawn to a need for caution in the thermodynamic characterization of nonspecific binding of a large ligand to a linear acceptor such as a polynucleotide or a polysaccharide—because of the potential for misidentification of a transient (pseudoequilibrium) state as true equilibrium. The time course of equilibrium attainment during the binding of a large ligand to nonspecific three-residue sequences of a linear acceptor lattice has been simulated, either by numerical integration of the system of ordinary differential equations or by a Monte Carlo procedure, to identify the circumstances under which the kinetics of elimination of suboptimal ligand attachment (called the parking problem) create such difficulties. These simulations have demonstrated that the potential for the existence of a transient plateau in the time course of equilibrium attainment increases greatly (i) with increasing extent of acceptor saturation (i.e., with increasing ligand concentration), (ii) with increasing magnitude of the binding constant, and (iii) with increasing length of the acceptor lattice. Because the capacity of the polymer lattice for ligand is most readily determined under conditions conducive to essentially stoichiometric interaction, the parameter so obtained is thus likely to reflect the transient (irreversible) rather than equilibrium binding capacity. A procedure is described for evaluating the equilibrium capacity from that irreversible parameter; and illustrated by application to published results [M. Nesheim, M.N. Blackburn, C.M. Lawler, K.G. Mann, J. Biol. Chem. 261 (1986) 3214–3221] for the stoichiometric titration of heparin with thrombin.

Keywords: Protein–polymer interactions; Nonspecific binding; Parking problem kinetics; Thrombin–heparin interaction

1. Introduction

In interactions between protein ligands and linear polymeric acceptors such as polynucleotides [1,2] or polysaccharides [3], a complication arises whenever the site for ligand binding comprises a sequence of two or more consecutive residues on the polymer chain (lattice). Because of the similarity of the re-

* Corresponding author. Department of Biochemistry, University of Queensland, Brisbane, Queensland 4072, Australia. Fax: +61-7-3365 2132; e-mail: winzor@biosci.uq.edu.au

[1] Present address: Department of Biochemistry and Molecular Biophysics, Washington University School of Medicine, St. Louis, MO 63110.

0301-4622/98/$19.00
PII S0301-4622(98)00104-5

peating units of the linear lattice, there may be no specific site for binding: any residue sequence of the appropriate length is a potential site for ligand attachment, resulting in a readily definable, albeit complicated case of bona fide nonspecific binding. During the early stages of such nonspecific binding, the random attachment of ligand molecules leads to the existence on the acceptor chain of spaces between bound ligands that contain too few residues to accommodate an additional ligand molecule. This is despite the fact that there would be sufficient unoccupied residues if the bound molecules were aligned laterally in an optimal arrangement. This feature is illustrated in Fig. 1 for the binding of a ligand to three-residue sequences of a 17-unit lattice. Clearly, the maximum number of ligand molecules that can attach to the chain is five (Fig. 1a); but if random binding leads to the distribution of the first four ligands shown in Fig. 1b, this chain is effectively saturated with only four ligand molecules until the combined processes of dissociation and association result in the required optimal alignment of bound ligand molecules so that another vacant three-residue sequence is created. Fig. 1c represents an even more extreme situation wherein effective saturation of the lattice is achieved after the attachment of only three ligand molecules. From the thermodynamic viewpoint the latter two examples are not equilibrium situations because they merely represent transient states on the route to chain saturation with five ligand molecules. Because we shall be considering later the possibility that ligand occupies more lattice sites than the number to which it actually binds, the corresponding transient parking problem is illustrated for a symmetrical overlap situation entailing interaction with three but occupancy of five lattice sites (Fig. 1d,e): transient saturation states with two rather than three bound ligand molecules can clearly be formed.

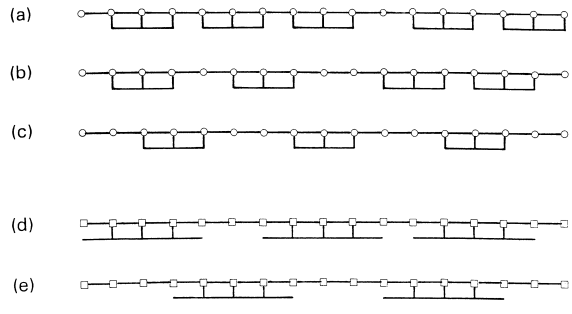

Fig. 1. Schematic representation of three 'saturated' complexes, (a)–(c), formed during the early stages of random attachment of a ligand [S] to three-residue sequences on a 17-residue acceptor lattice [A]: (b) and (c) are transient states that are eliminated in the attainment of equilibrium. Panels (d) and (e) illustrate examples of equilibrium and transient saturation states respectively for a ligand that binds to three ($n = 3$) but occupies five ($m = 5$) lattice units.

Operationally, an equilibrium situation is assumed to exist when no significant change in binding with time can be observed. In the systems under consideration, the transient parking problem is shown to increase with increasing ligand concentration, the suboptimal occupation of sites being maximal under conditions approaching saturation of acceptor with ligand. However, inspection of the quantitative expressions for the nonspecific interaction of ligands with segments of a linear polymer [2,4–7] clearly indicates that suboptimal use of sites, termed the parking problem [8,9], is eliminated in the limit of infinite ligand concentration for accurate thermodynamic description of the binding process. The matter addressed in this investigation is the time-course of the elimination of the parking problem, which can be a key issue in the collection of binding data, particularly by spectrophotometric or spectrofluorometric titration.

Major contributions to our understanding of nonspecific binding to one-dimensional lattices of finite length have been provided by Epstein et al. [5,10–15]. In their examination of the kinetics of the binding process, Monte Carlo methods were used for 'exact' numerical simulations, whereas approximate analytical solutions were obtained by assuming that the extent of ligand binding had no effect on the free concentration of ligand. The use of numerical methods to solve the system of ordinary differential equations describing the kinetics was raised but deemed impractical because of the number of differential equations to be solved. Developments in computer software technology have alleviated that impediment.

In the present investigation, advantage is taken of a commercial software package to simulate numerically the solution of the set of ordinary differential equations describing the kinetics of nonspecific binding of ligands to one-dimensional lattices. These computer-simulated time-courses of the approach to thermodynamic equilibrium provide valuable insight

into the identification of conditions under which kinetic aspects of the parking problem have the potential to interfere with the thermodynamic characterization of nonspecific binding to sequences of consecutive residues on a linear lattice. On the grounds that considerable difficulty is likely to be encountered in deducing the maximum number of polymer sites available for ligand binding from equilibrium measurements, a procedure is described for determining this parameter on the basis of the endpoint of a titration performed under conditions of stoichiometric complex formation.

2. Methods

As mentioned above, evaluation of the time course of equilibrium attainment has involved the establishment of systems of ordinary differential equations for the binding of ligands which cover three consecutive residues on linear acceptors ranging from six to nine residues in length. These differential equations were solved by means of the SCIENTIST modelling package from Micromath Scientific Software (Salt Lake City, UT) operating on a 486 PC. The numerical technique used most often to integrate the differential equations was EPISODE, an Adams–Moulton type method for stiff equations that is available as an option on the SCIENTIST menu. This program provided a faster return of the solution (order of a minute) than could be accomplished by means of alternative options based on the Bulirsch-Stoer and Runge Kutta algorithms. Thus, despite the fact that none of the sets of differential equations comprised stiff systems, EPISODE was used to explore the conditions that give rise to parking problem kinetics that could impede and confound the experimental measurement of thermodynamic binding data.

The simulations model the time dependence of acceptor occupancy, defined in the usual way as the ratio of the concentration of ligand bound to the total concentration of acceptor. This binding function, r_t, which is given a subscript to denote its time dependence, ranges from zero (at $t = 0$) to an equilibrium value, r_{eq}. Values of r_t have been determined by following the variation of the free ligand concentration at time t, $[S]_t$, in a mixture with total concentrations $[A]_{tot}$ and $[S]_{tot}$ of acceptor and ligand, respectively, and then calculating the binding function as

$$r_t = ([S]_{tot} - [S]_t)/[A]_{tot} \quad (1)$$

2.1. The set of ordinary differential equations

The method of constructing a system of ordinary differential equations for the binding of a large ligand to a linear lattice is illustrated by considering the interactions of a ligand with any three consecutive residues of a seven-residue lattice under conditions where the same association and dissociation rate constants apply to all interactions. The relevant features of the approach are summarized in Fig. 2. For this situation there are clearly five positions available for attachment of the first ligand molecule, all of which are equally probable. In addition to these five species, designated ^{1}AS to ^{5}AS , there are three

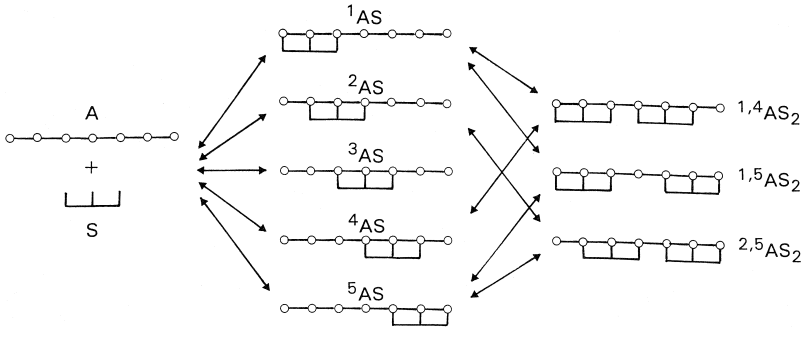

Fig. 2. Schematic representation of the various acceptor–ligand complexes formed in the nonspecific binding of a ligand [S] to three-residue sequences on an acceptor lattice [A] comprising seven residues. Arrows indicate the interconversion of the various acceptor–ligand species resulting from attachment or removal of ligand.

species, $^{1,4}AS_2$, $^{1,5}AS_2$, and $^{2,5}AS_2$, that can be formed by attaching a second ligand molecule. Formation of each of these species can occur in two ways (Fig. 2), the order of attachment being immaterial to the thermodynamic definition of the species.

In constructing the system of ordinary differential equations it is necessary to consider the formation and loss of the relevant species. For example, in writing the expression for $d[S]/dt$ account needs to be taken of (i) the decrease in the concentration of free ligand concentration, [S], as the result of ligand binding to various acceptor species, and (ii) the increase in [S] resulting from detachment of ligand from acceptor–ligand complexes. It needs to be noted that there are five ways of attaching a ligand molecule [S] to naked lattice [A], two ways of attaching [S] to ^{1}AS and ^{5}AS, and one way of attaching ligand to ^{2}AS and ^{4}AS. Likewise, it is necessary to take into account the fact that the dissociation of each of the 1:1 acceptor–ligand complexes (^{1}AS to ^{5}AS) releases a free ligand molecule; and that in the same time period $^{1,4}AS_2$, $^{1,5}AS_2$ and $^{2,5}AS_2$ serve as the source of two free ligand molecules. The consequent expression is presented as the first entry in Table 1, which summarizes the complete set of ordinary differential equations, in which k_f and k_r are used to denote the respective association (forward) and dissociation (reverse) rate constants for the noncooperative acceptor–ligand interaction.

Two important points emerge from this set of ordinary differential equations. First, although there are 10 equations (one for each species), the symmetry of the system is such that three are effectively duplicated, thereby decreasing the number of independent differential equations to be solved simultaneously. For example, ^{4}AS formation from and dissociation into [A] and [S] gives rise to the terms $k_f[A][S] - k_r[^4AS]$ in the expression for $d[^4AS]/dt$, whereas the formation and breakdown of the doubly-liganded complex $^{1,4}AS_2$ yields the terms $-k_f[^4AS][S] + k_r[^{1,4}AS_2]$. However, simulations run with the differential equation for ^{4}AS expressed in these terms exactly match the concentration of ^{2}AS because of the geometric symmetry of the ligand positions. Similarly, ^{1}AS and ^{5}AS, as well as $^{1,4}AS_2$ and $^{2,5}AS_2$, share common solutions. Such symmetry considerations can become important because the SCIENTIST package has an upper limit of 100 differential equations for simultaneous solution. The second point to note in relation to Table 1 is that the simpler form of the differential equation for ^{3}AS reflects the inability of this species to bind a second molecule of ligand. More optimal ligand uptake by a polymer chain complexed in this fashion is thus reliant upon prior dissociation to reform naked lattice [A], for which there is an 80% chance of an initial ligand attachment that is conducive to the binding of a second molecule of ligand.

Table 1
System of ordinary differential equations for noncooperative binding of ligand [S] to three-residue sequences of an acceptor [A] comprising seven residues

Species (i)[a]	$d[i]/dt$[b]
S	$-5k_f[A][S] + k_f([^1AS] + [^2AS] + [^3AS] + [^4AS] + [^5AS]) - k_f[S](2[^1AS] + [^2AS] + [^4AS] + 2[^5AS]) + 2k_r([^{1,4}AS_2] + [^{1,5}AS_2] + [^{2,5}AS_2])$
A	$-5k_f[A][S] + k_r([^1AS] + [^2AS] + [^3AS] + [^4AS] + [^5AS])$
^{1}AS	$k_f[A][S] - k_r[^1AS] - 2k_f[S][^1AS] + k_r([^{1,4}AS_2] + [^{1,5}AS_2])$
^{2}AS	$k_f[A][S] - k_r[^2AS] - k_f[S][^2AS] + k_r[^{2,5}AS_2]$
^{3}AS	$k_f[A][S] - k_r[^3AS]$
^{4}AS[c]	$d[^2AS]/dt$
^{5}AS[c]	$d[^1AS]/dt$
$^{1,4}AS_2$	$k_f[S]([^1AS] + [^4AS]) - 2k_r[^{1,4}AS_2]$
$^{1,5}AS_2$	$k_f[S]([^1AS] + [^5AS]) - 2k_r[^{1,5}AS_2]$
$^{2,5}AS_2$[c]	$d[^{1,4}AS_2]/dt$

[a] Acceptor–ligand complex species are defined in Fig. 1.
[b] Association and dissociation rate constants are denoted by k_f and k_r, respectively.
[c] Species for which the differential equation is identical with that for another species.

2.2. Monte Carlo simulations

Progress curves for the binding of large ligands to consecutive residues of a linear acceptor lattice have also been obtained by Monte Carlo type simulations on a massively parallel computing facility (MasPar Computer, Sunnyvale, CA), which allowed the computing time for this type of simulation to be decreased from days to 7 h of single-user time. A program, written in MasPar Fortran, has been developed such that it operates in parallel on two-dimensional arrays of the order of 1000×10 elements. The binding process was simulated as random attachment and detachment of ligands to/from acceptor residues, the random number generator of the computer being used to select the acceptor residues for any given event (attachment or detachment). This Monte Carlo method was used to model binding to three-residue sequences on linear acceptors ranging from 6 to 14 residues in length.

The decision to switch from numerical solution of the system of ordinary differential equations reflected an upper limit of 10 for the number of differential equations that could be solved by the software package available at that time. In retrospect, resort to Monte Carlo simulations could have been avoided because of a 10-fold increase in the number of ordinary differential equations amenable to simultaneous solution by current SCIENTIST software. However, the demonstration of agreement between solutions obtained by the two procedures has provided an important check on the validity of solutions obtained by either procedure. In that regard the long time (many hours) required to establish a time course of ligand binding by Monte Carlo simulation is clearly a disadvantage from the viewpoint that the same information could have been obtained in a minute by the alternative procedure. On the other hand, this disadvantage is offset to some extent by the fact that there is less room for error in the change of program to accommodate a change in length of the acceptor. Because the system of ordinary differential equations needs to be established ab initio for each linear lattice, extreme care is required to ensure the correctness of sets of differential equations such as those presented in Table 1. Confirmation of the simulated progress curve by this independent procedure thus provides additional assurance that the particular system of ordinary differential equations is, indeed, correct.

2.3. Nonspecific binding with an irreversible parking problem

In previous studies of the nonspecific binding of a ligand to n-unit sequences of a polymer chain comprising N units, the randomness of initial ligand attachment has been considered to be eliminated in the limiting situation of acceptor saturation with ligand. This thermodynamically rigorous definition of the reaction stoichiometry as the integer value (R) of N/n is therefore conditional upon the lapse of a sufficient time period for the dissociation and relocation of inefficiently parked ligand molecules. However, the time scale of an experiment may not allow the occurrence of sufficient dissociation and reassociation events to effect the rearrangement of bound ligand molecules that is required for attainment of the capacity (stoichiometry) predicted on thermodynamic grounds.

The present stance is similar to that adopted by Flory [16] in assessing the stoichiometry of irreversible condensation of adjacent functional sidegroups on a linear polymer; but differs therefrom in two respects. First, binding to larger lattice segments is also considered. Secondly, the concept of equilibrium between free and bound states is presumed to prevail despite the fact that inefficient parking of ligand has temporarily masked the existence of some potential sites on the polymeric acceptor. Although indefensible on rigorous thermodynamic grounds, such a concept of pseudoequilibrium should apply when there is a slow coalescence of isolated lattice units to form the n-unit segment required for binding of an additional ligand molecule. This suboptimal, pseudoequilibrium capacity is observed as a transient plateau in simulated time courses of equilibrium attainment (see later). Furthermore, the equivalence of this transient capacity and that determined for irreversible binding has also been demonstrated. The theory of irreversible binding has therefore been utilized to determine expressions for the pseudoequilibrium capacity.

Recursive argument is used to determine the irreversible capacities of linear lattices of identical units. For each point of first attachment the lattice has the

potential to support one ligand molecule plus the capacities of the sublattices on either side of that position [5]. The total number of attached ligands, calculated by considering all points of first attachment plus the consequent sublattice capacities, is averaged over the number of points of initial attachment to give the irreversible capacity. The recursive relationship describing the irreversible capacity, $(R_i)_N$ of an N-unit lattice for a ligand binding to n units is

$$(R_i)_N = 1 + \left\{ 2 \sum_{L=1}^{N-n} (R_i)_L \right\} / (N - n + 1) \qquad (2)$$

where $(R_i)_L$ is the irreversible capacity of a sublattice with L units. Initial terms of the recursive relation are simply determined by considering that the lattice (sublattice) length must be at least as large as the number of units involved in attachment of ligand for binding to occur; and that lattices with a length less than twice that span can only bind one ligand molecule. Further development of the logic behind the recursive formula is most readily illustrated by means of a specific example.

Consider, as illustrated in Fig. 3, the attachment of the first ligand molecule to a three-unit segment of a lattice with 10 units ($N = 10$). If the ligand molecule is attached to the first three units (species A), there are no units to its left for further attachments; but there are still seven units to its right. On the other hand, attachment of the first ligand molecule to positions 4–6 (species D) leaves available a sublattice with three units to the left and one with four units to the right. The irreversible capacities of each of the sublattices, $(R_i)_L$, now need to be determined.

From the above discussion it follows that $(R_i)_0 = (R_i)_1 = (R_i)_2 = 0$, and that $(R_i)_3 = (R_i)_4 = (R_i)_5 = 1$; but we now need to resort to further recursive argument (Eq. (2)) to obtain values of $(R_i)_6$ and $(R_i)_7$. Specifically, $(R_i)_6 = 1 + 2(R_i)_3/4 = 1.5$; and $(R_i)_7 = 1 + 2[(R_i)_3 + (R_i)_4]/5 = 1.8$. The irreversible capacity of this 10-unit lattice for a ligand attaching to three-unit segments thus becomes $(R_i)_N = 1 + 2[(R_i)_3 + (R_i)_4 + (R_i)_5 + (R_i)_6]/8 = 2.575$, which is only 86% of the capacity ($R = 3$) if binding were allowed to attain thermodynamic equilibrium. Table 2 lists the chainlength dependence of the irreversible capacity for a ligand that binds non-

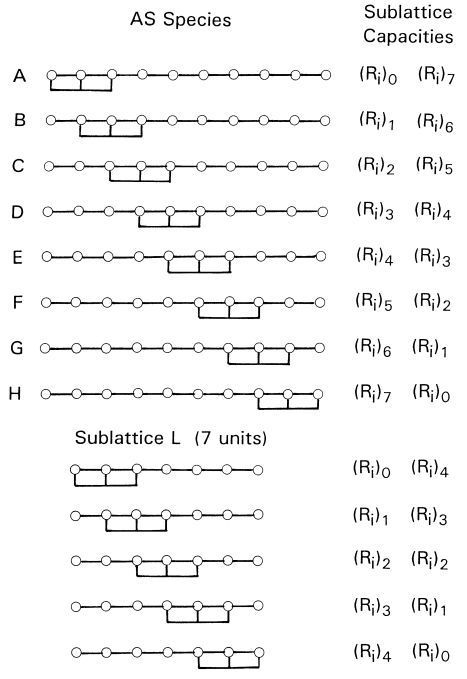

Fig. 3. Schematic representation of possible initial attachments in the irreversible binding of ligand to three-unit segments ($n = 3$) of a 10-unit lattice ($N = 10$) to show the sublattice formation from which the capacity is deduced by recursive logic on the basis of Eq. (2).

specifically to sequences of two to eight units of lattices with up to 40 units.

Provided that the overlap is symmetrical, similar reasoning for the situation in which ligand occupies m while only binding to n lattice units (Fig. 1d,e) leads to the expression

$$(R_i)_N = 1 + \left\{ 2 \sum_{L=1}^{N-m} (R_i)_L \right\} / (N - n + 1) \qquad (3)$$

for the irreversible relationship. On the grounds that the only difference between Eqs. (2) and (3) is the upper limit of the summation, the irreversible capacity for such a system may also be obtained as the appropriate entry in Table 2 for an acceptor with $N + (m - n)$ units. For example, the irreversible capacity of a 20-unit lattice for a ligand that binds to three but occupies five units (a 5_3 ligand) is 3.28, the entry in Table 2 for $n = 5$ and $N = (20 + 5 - 3) = 22$. This conclusion finds quantitative parallel in

Table 2
Dependence, upon polymer chainlength (N), of the irreversible capacity of an acceptor lattice for nonspecific binding of a ligand to a segment of n residues

N	Irreversible capacity (R_i)						
	$n=2$	$n=3$	$n=4$	$n=5$	$n=6$	$n=7$	$n=8$
1	0.00	0.00	0.00	0.00	0.00	0.00	0.00
2	1.00	0.00	0.00	0.00	0.00	0.00	0.00
3	1.00	1.00	0.00	0.00	0.00	0.00	0.00
4	1.67	1.00	1.00	0.00	0.00	0.00	0.00
5	2.00	1.00	1.00	1.00	0.00	0.00	0.00
6	2.47	1.50	1.00	1.00	1.00	0.00	0.00
7	2.89	1.80	1.00	1.00	1.00	1.00	0.00
8	3.32	2.00	1.40	1.00	1.00	1.00	1.00
9	3.76	2.29	1.67	1.00	1.00	1.00	1.00
10	4.19	2.58	1.86	1.33	1.00	1.00	1.00
11	4.62	2.84	2.00	1.57	1.00	1.00	1.00
12	5.05	3.12	2.20	1.75	1.29	1.00	1.00
13	5.48	3.39	2.41	1.89	1.50	1.00	1.00
14	5.92	3.67	2.62	2.00	1.67	1.25	1.00
15	6.35	3.94	2.82	2.15	1.80	1.44	1.00
16	6.78	4.22	3.02	2.32	1.91	1.60	1.22
17	7.21	4.49	3.22	2.49	2.00	1.73	1.40
18	7.65	4.77	3.42	2.65	2.12	1.83	1.55
19	8.08	5.04	3.62	2.81	2.26	1.92	1.67
20	8.51	5.31	3.82	2.96	2.39	2.00	1.77
21	8.94	5.59	4.02	3.12	2.53	2.10	1.86
22	9.38	5.86	4.23	3.28	2.67	2.21	1.93
23	9.81	6.14	4.43	3.44	2.80	2.33	2.00
24	10.24	6.41	4.63	3.60	2.92	2.45	2.08
25	10.67	6.69	4.83	3.75	3.05	2.56	2.18
26	11.11	6.96	5.03	3.91	3.18	2.68	2.28
27	11.54	7.24	5.23	4.07	3.31	2.79	2.38
28	11.97	7.51	5.43	4.23	3.45	2.90	2.49
29	12.40	7.79	5.63	4.39	3.58	3.01	2.59
30	12.83	8.06	5.83	4.55	3.71	3.12	2.69
31	13.27	8.33	6.03	4.70	3.84	3.23	2.78
32	13.70	8.61	6.24	4.86	3.97	3.34	2.88
33	14.13	8.88	6.44	5.02	4.10	3.45	2.97
34	14.56	9.16	6.64	5.18	4.23	3.56	3.07
35	15.00	9.43	6.84	5.34	4.36	3.68	3.17
36	15.43	9.71	7.04	5.50	4.49	3.79	3.26
37	15.86	9.98	7.24	5.66	4.62	3.90	3.36
38	16.29	10.26	7.44	5.81	4.75	4.01	3.46
39	16.73	10.53	7.64	5.97	4.88	4.12	3.55
40	17.16	10.81	7.84	6.13	5.02	4.23	3.65

thermodynamic studies, which are based on a reversible capacity of $(N+m-n)/m$ to account for the fact that a ligand molecule attached to the terminal region of an acceptor can protrude beyond the end of a chain and hence occupy fewer than m sites [5].

3. Results

3.1. Comparison of simulated progress curves

The excellent agreement between results from the two procedures used to simulate the time course of equilibrium attainment is illustrated in Fig. 4, which compares progress curves obtained by the EPISODE numerical integration procedure (————) with those obtained by Monte Carlo simulation (symbols) for the binding of a large ligand to three consecutive residues on a seven-residue lattice. Confidence in the validity of such simulated time courses is obviously enhanced by independence of the result upon the method of generation. Time courses of acceptor occupancy (r_t) and free ligand concentration ($[S]_t$) are presented in Fig. 4a for a reaction mixture with 2.4

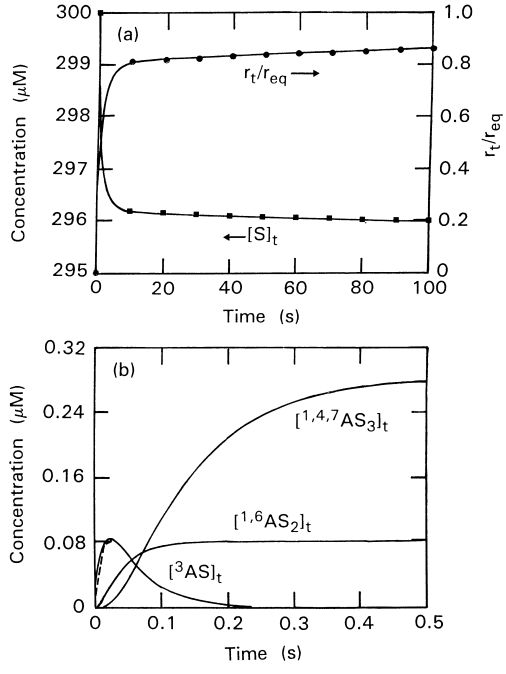

Fig. 4. Comparison of progress curves obtained by numerical integration (EPISODE program) of the system of ordinary differential equations (————) and by Monte Carlo simulations (symbols) for the nonspecific interaction of ligand [S] with three-residue sequences of a seven-residue acceptor lattice [A] governed by association and dissociation rate constants (k_f, k_r) of 0.001 μM^{-1} s^{-1} and 0.01 s^{-1}, respectively: values of 2.4 μM and 300 μM were assigned to the respective total concentrations of acceptor ($[A]_{tot}$) and ligand ($[S]_{tot}$). (a) Time dependence of the concentration of free ligand (■) and the binding function (●). (b) Corresponding time courses for the concentrations of the indicated acceptor–ligand complexes (see Fig. 2 for terminology).

μM acceptor ($[A]_{tot}$), 300 μM ligand ($[S]_{tot}$) and noncooperative binding governed by association and dissociation rate constants of 0.001 μM^{-1} s^{-1} and 0.01 s^{-1}, respectively: time courses for the concentrations of ^{2}AS, ^{3}AS, and $^{1,5}AS_2$ are presented in Fig. 4b: magnitudes of parameters (r_t, $[S]_t$, $[^{1,5}AS_2]_t$) at $t = 1000$ s, are indistinguishable from the equilibrium values. The concentrations of ^{3}AS and ^{2}AS at 1000 s are identical and essentially equal to the magnitude of $[^{2}AS]_t$ attained within the first 10 s of reaction.

The reason for relatively slow attainment of thermodynamic equilibrium becomes evident from considering the various progress curves presented in Fig. 4. For this system there is an extremely fast decrease in the concentration of free ligand in the first 10 s of reaction, after which $[S]_t$ continues to decline slowly for about 10 min: this time course is necessarily mirrored in the average occupancy (r_t), which only attains its equilibrium value after 10 min despite reaching 90% of that value within the first 10 s (Fig. 4a). Inspection of the progress curves for individual species (Fig. 4b) shows that the slow kinetic phase reflects the necessity of depleting the concentration of ^{3}AS from that formed initially in order to achieve a concentration of ligand-saturated complexes ($^{1,4}AS_2$, $^{1,5}AS_2$ and $^{2,5}AS_2$) that is in thermodynamic equilibrium with the other species. Thus, whereas the concentrations of those species which are compatible with the direct formation of saturated complex attain their equilibrium values within the first few seconds of reaction ($^{1}AS \rightarrow {}^{1,4}AS_2$ and $^{1,5}AS_2$; $^{2}AS \rightarrow {}^{2,5}AS_2$), the formation of ^{3}AS is incompatible with formation of a saturated complex. Inasmuch as the formation of additional saturated complexes is conditional upon the dissociation of ^{3}AS, the slow phase in the time course for the concentrations of these saturated species mirrors that of the decline in $[^{3}AS]$. Persistence of the slow phase of the parking problem kinetics thus correlates with the proportion of unsaturable acceptor–ligand complexes for a linear acceptor of given length.

3.2. Conditions conducive to significant parking problem kinetics

The chief goal of this investigation has been the delineation of conditions under which kinetic aspects of the elimination of the parking problem are most likely to bring into question the validity of subjecting experimental measurements to analysis in terms of binding equations based on the premise of equilibrium attainment. On the grounds that the extent of acceptor saturation is likely to be a key issue, we first examine (Fig. 5a) the effect of total ligand concentration, $[S]_{tot}$, on the time course of equilibrium attainment for a system in which the binding of ligand to three-residue sequences on a six-residue acceptor lattice ($[A]_{tot} = 1$ μM) is governed by respective association and dissociation rate constants of 0.001 μM^{-1} s^{-1} and 0.01 s^{-1}, the values that had been assigned to these parameters in the simulations presented in Fig. 4. As the total ligand concen-

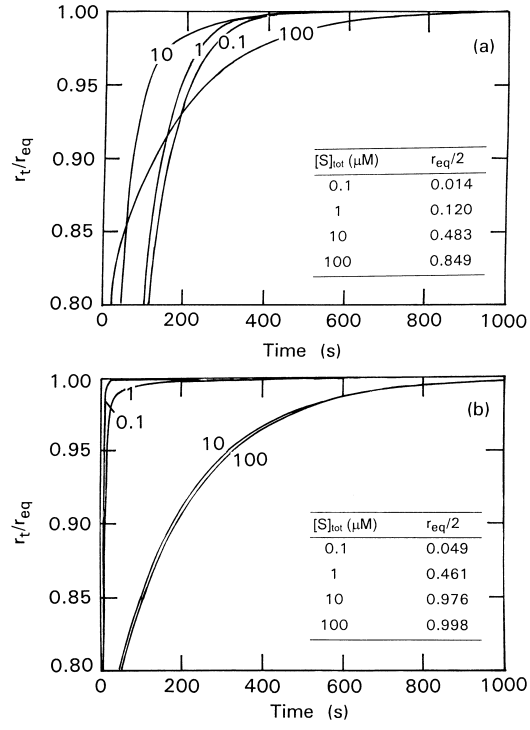

Fig. 5. Time dependence of the binding function, expressed as a proportion of the equilibrium value, from simulations of the nonspecific binding of ligand to three-residue sequences of a six-residue acceptor lattice in situations with $[A]_{tot} = 1$ μM, the indicated concentrations (μM) of ligand ($[S]_{tot}$), a dissociation rate constant (k_r) of 0.01 s^{-1}, and (a) $k_f = 0.001$ μM^{-1} s^{-1}; (b) $k_f = 0.1$ μM^{-1} s^{-1}. The inserts show the fractional saturation at equilibrium for the given total ligand concentration ($[S]_{tot}$): to obtain the fractional saturation at equilibrium, r_{eq} is divided by 2, the saturating number of ligand molecules R in this system.

tration is increased from 0.1 μM to 10 μM, the time to reach 98% of equilibrium occupancy decreases progressively; but this trend is reversed when $[S]_{tot}$ is increased to 100 μM. In the low range of ligand concentration, for which binding at equilibrium corresponds to 1.4 to 48% saturation of acceptor (tabulated in Fig. 5a), the faster rate of equilibrium attainment with increasing ligand concentration conforms with second-order kinetic behavior for the association reaction. As predicted on that basis, an even faster rate of binding applies to the initial stages of the progress curve for the highest ligand concentration, which gives rise to 85% saturation of acceptor at equilibrium; but the kinetics of parking problem elimination then assume control of the overall approach to equilibrium. The simulated results presented in Fig. 4a thus confirm intuitive reasoning by establishing that parking problem kinetics are unlikely to be a cause for concern in the experimental collection of equilibrium binding data at low levels of acceptor saturation, but that they do prolong considerably the time required to acquire measurements reflecting equilibrium in mixtures with a high level of acceptor saturation.

It can certainly be argued that the simulations presented in Fig. 5a refer to a situation in which the association rate constant is several orders of magnitude below the level of diffusion control; and that equilibrium for an experimental system with a binding constant (k_f/k_r) of 10^5 M^{-1} could well be attained much more quickly than is suggested by these simulated progress curves. To encompass the fact that much larger intrinsic binding constants frequently prevail in protein–polymer interactions, Fig. 5b presents the results of corresponding simulations for the same system with k_f increased 100-fold to 0.1 μM^{-1} s^{-1}, a more likely value ($K = 10^7$ M^{-1}). Equilibrium is again attained rapidly at the lowest ligand concentration (0.1 μM), but the kinetics of the parking problem are already becoming evident in the simulated time course for 1 μM ligand.

The simulated results presented in Fig. 5a serve as a warning to experimenters of the need to ascertain whether a seemingly stable spectrophotometric or spectrofluorometric signal reflects equilibrium attainment or merely the onset of the slow phase of the progress curve. The observation that kinetic effects of the parking problem can be minimized by restricting measurements of ligand binding to low levels of acceptor saturation is not the solution to an experimenter's dilemma, unless the size of the residue sequence for ligand attachment can be ascertained by other means. A lack of data in the second half of a binding curve clearly precludes unequivocal experimental delineation of the binding capacity of the acceptor, which is the key indicator of the size of the residue sequence occupied by a ligand molecule, and hence the determinant of the binding equation used to analyze the experimental results.

The factor that determines whether or not kinetic aspects of the elimination of the parking problem are likely to be a major consideration in experimental studies of nonspecific ligand binding under conditions of high acceptor concentration is, of course, the magnitude of the dissociation rate constant, which dictates the rate of equilibrium attainment because it governs the breakdown of unsaturable acceptor–ligand complexes (^{3}AS in Fig. 3b). This influence of k_r is emphasized in Fig. 6, which presents the results of simulations with $[S]_{tot} = 100$ μM and $[A]_{tot} = 1$ μM (as in Fig. 5b) for systems in which the binding of ligand to three-residue sequences of a six-residue lattice is governed by an association rate constant (k_f) of 0.1 μM^{-1} s^{-1} and a 100-fold range of dissociation rate constants: by expressing the abscissa as the logarithm of time, any persistence of a

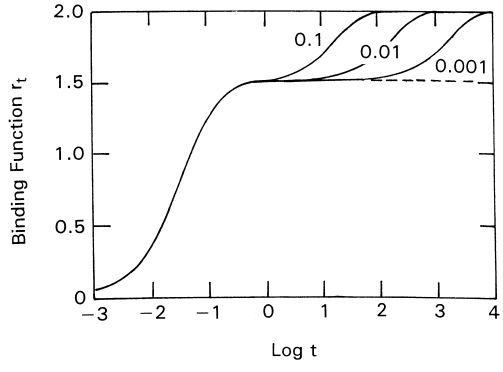

Fig. 6. Logarithmic time dependence (t in s) of the approach to equilibrium predicted by simulations of the nonspecific interaction between ligand and three-residue sequences of a six-residue acceptor lattice in situations with $[A]_{tot} = 1$ μM, $[S]_{tot} = 100$ μM, $k_f = 0.1$ μM^{-1} s^{-1} and the indicated magnitudes (s^{-1}) for the dissociation rate constant (k_r): the broken line signifies irreversible binding ($k_r = 0$).

pseudoequilibrium plateau is highlighted. For the system with a binding constant of 10^6 M^{-1} ($k_r = 0.1$ s^{-1}) the parking problem would be unlikely to impede measurement of an equilibrium response, which is attained within 2 min. For the system with a binding constant of 10^8 M^{-1} ($k_r = 0.001$ s^{-1}), however, the parking problem is only eliminated after 2.5 h despite the fact that a seemingly stable plateau response would have been observed within a second of mixing the reactants. This observation is very sobering from the viewpoint that one experimental approach to defining the acceptor capacity for ligand entails measurement of ligand binding under conditions where reaction is essentially stoichiometric. Selection of reaction conditions (a change in pH or a lower ionic strength) that enhance the magnitude of the binding constant virtually guarantees a decrease in k_r, and hence exacerbates the problem of obtaining a binding response that reflects thermodynamic equilibrium.

The validity of the prediction that persistence of the parking problem should correlate with the proportion of unsaturable complexes is borne out by the results of simulations presented in Fig. 7 for the binding of ligand to three-residue sequences on lattices comprising 6 to 14 residues: although these results were inferred from Monte Carlo simulations, we have confirmed the identity of predictions obtained by numerical integration for lattices comprising six to nine residues. In order to facilitate comparisons, the association and dissociation rate constants have been assigned fixed values of 0.001 μM^{-1} s^{-1} and 0.01 s^{-1} (as in Fig. 4). The total concentration of ligand, $[S]_{tot}$, has been fixed at 300 μM, while that of acceptor ($[A]_{tot}$) was assigned a magnitude of 3.0 μM in the simulations for a six-residue acceptor. Corresponding values for larger lattices were scaled down on the basis of the number of ways of initial attachment of ligand to an acceptor of given length relative to that (4 ways) for forming 1:1 complex on a 6-residue acceptor. There is a cyclical trend in the time required for equilibrium attainment, which goes through a maximum for lattice lengths that are multiples of the number of lattice residues occupied by a single ligand molecule, these being the lattices that give rise to the greatest proportion of unsaturable acceptor–ligand complexes. Another feature to be noted from Fig. 7 in addition to this cyclical fluctuation in time required for equilibrium attainment is the fact that the equilibration times exhibit a general increase with increasing acceptor length. This is evident from the final panel in Fig. 7, which avoids the distraction of the cyclical trend by comparing the time courses of equilibrium attainment for the three lattice lengths that are multiples of the three-residue sequence occupied by ligand. In an experimental context the difficulties associated with defining the thermodynamic endpoint of an acceptor–ligand titration are exacerbated by increasing length of the acceptor lattice because of the extension of the time required to eliminate the parking problem.

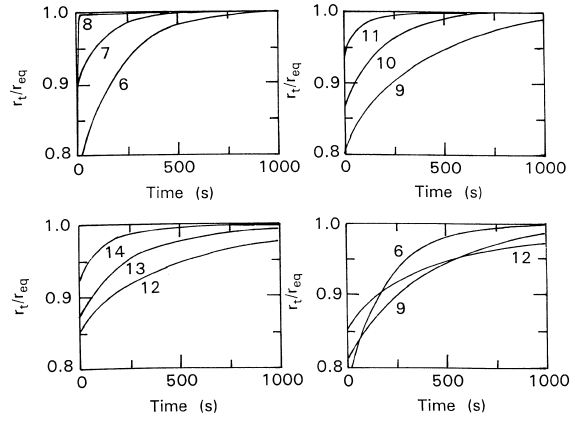

Fig. 7. Effect of acceptor chainlength on the time course of equilibrium attainment in numerical simulations of the nonspecific binding of ligand to three-residue sequences that is governed by association and dissociation rate constants of 0.001 μM^{-1} s^{-1} and 0.01 s^{-1}, respectively, in mixtures with a total ligand concentration ($[S]_{tot}$) of 300 μM. The total concentration of acceptor ($[A]_{tot}$), which was 3 μM for the six-residue lattice, was scaled down in accordance with the number of ways of forming 1:1 complex with the lattice, which ranged in length from 6 to 14 residues (number against each progress curve).

At first sight it might seem that any underestimation of the maximal value of the binding function ($r_{eq} = R$) would be recognized immediately on the basis that the capacity must be an integer for a lattice with a given chainlength. However, because polymer lattices will generally exhibit polydispersity with respect to chainlength, the determination of a non-integer value for R is likely to be attributed to that cause rather than to underestimation of the capacity. A consequent misidentification of the number of residues spanned by a single ligand molecule would

then be incorporated into the thermodynamic expression used to interpret the valid equilibrium binding data obtained at lower extents of lattice saturation. To avoid such pitfalls, it can be argued that a more appropriate avenue of attack on the reaction stoichiometry from such measurements would be to interpret the experimentally measured pseudoequilibrium plateau response as though the parking problem were irreversible—a procedure now illustrated by considering results for the interaction of thrombin with heparin.

3.3. The interaction of thrombin with heparin

In this section we make use of results from a spectrofluorometric study [17] of the interaction between thrombin and heparin, a polysaccharide in which the repeat unit is a disaccharide comprising α-L-iduronic acid-2-sulfate linked β-1,4 to *N*-sulfurylglucosamine-6-sulfate. Nesheim et al. [17] adopted the direct approach to the capacity question by titrating dansylated thrombin with heparin under conditions conducive to effectively stoichiometric reaction (Fig. 8a). The consequent results for the dependence of heparin capacity for thrombin upon molecular weight of the polysaccharide are summarized (■) in Fig. 8b, where the abscissa has been converted to the number of disaccharide units (N) on the basis of a molecular weight of 615 for the repeating disaccharide unit [3]. In the sense that the capacity extrapolates to a value of unity for $N = 3$, these results are seemingly consistent with the conclusion [3] that thrombin binds nonspecifically to a linear sequence of three, rather than two [18] disaccharide units. However, the predicted chainlength dependence, as shown by the step function in Fig. 8b, provides an extremely poor description of the experimental results. We therefore take note of the statement [17] that subsequent addition of unlabelled thrombin failed to affect the extent of fluorescence quenching already measured for a given mixture of heparin and dansylated thrombin. Although the authors were at a loss to account for this result so out of keeping with their expectation, a plausible explanation is that a slow dissociation rate constant (consistent with the extremely large K that pertains in a stoichiometric titration) effectively precluded any dissociation of acceptor–ligand complex(es) in the relatively short time (order of 1 min) allowed for re-equilibration. The heparin capacity data are therefore considered in terms of titrations that reflect the irreversible (pseudoequilibrium) endpoints prior to elimination of the parking problem.

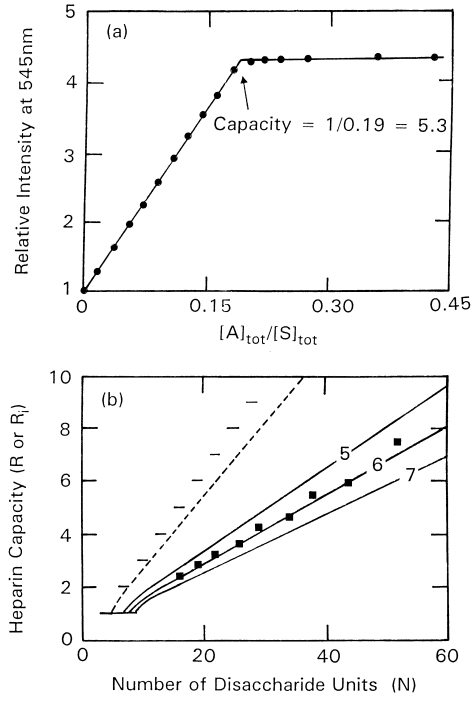

Fig. 8. Consideration of results from spectrofluorometric titrations of dansylated thrombin [S] with heparin [A] in terms of nonspecific binding. (a) Establishment of the essentially stoichiometric nature of the interaction from the form of the titration curve for a sample of heparin with a molecular weight (M_A) of 27,400. (b) Comparison of experimental results (■) with the chainlength dependence ($N = M_A/615$) of heparin capacity for thrombin predicted for various models of the nonspecific interaction: step function, thermodynamic capacity for ligand binding to three-unit segments; ---, corresponding dependence for irreversible binding to three-unit segments. Solid lines refer to models involving irreversible interaction with ($n = 3$) but occupancy of the indicated number (m) of disaccharide units of the *N*-unit heparin chain. Data in (a) and (b) are inferred from Figs. 5 and 6, respectively, of Ref. [17].

Little improvement in the degree of correspondence between prediction and experiment is effected by considering the titrations to yield the irreversible endpoint for noncooperative binding of thrombin to three-unit segments of the heparin chain (- - -). Adoption of the viewpoint that thrombin may be binding

to hexasaccharidic sequences ($n = 3$) but occupying larger segments ($m > n$) leads to the predicted chain-length dependencies of R_i designated by the solid lines in Fig. 8b for the indicated values of m. Interaction with three but occupancy of six disaccharide units (Eq. (3)) provides the best description of the stoichiometric titration data in terms of noncooperative, nonspecific binding. Although the concept of a ligand binding to three but overlapping six lattice units (a 6_3 ligand) seemingly contravenes the assumed symmetry of overlap (Fig. 1d,e) that is inherent in the deduction of Eq. (3), symmetrical overlap is still feasible in this instance because of the disaccharidic nature of the repeat unit in the heparin chain.

The postulated system with $m > n$ is certainly plausible on the basis of the relative dimensions of thrombin molecules and disaccharide units. From X-ray crystallographic studies thrombin is effectively a prolate ellipsoid of revolution with dimensions $4.5 \times 4.5 \times 5.0$ nm [19], whereas studies with charged polyanionic saccharides indicate that the linear dimension of a disaccharide unit is in the vicinity of 1.0–1.2 nm [20]. An overlap model in which thrombin binds directly to a sequence of three disaccharides but excludes the binding of additional thrombin to adjacent disaccharide units is thus entirely reasonable.

In relation to the interpretation of equilibrium binding data, the important lesson to draw from Fig. 8 is that the thermodynamic binding capacities would be higher than those measured by stoichiometric titration. For example, despite the fact that the measured capacity of the largest heparin lattice ($N = 52$) is less than 8, the predicted thermodynamic capacity of this lattice for a 6_3 ligand is 9. Alternatively, consideration of the measured capacity as the thermodynamic parameter $R = (N + m - n)/m$ leads to the conclusion that thrombin is a 7_3 ligand and that the capacity R is 8. Thus, even though equilibrium binding measurements are usually made under conditions where the kinetics of parking problem elimination is not an issue, their quantitative interpretation requires a value of R to be specified in the expression [5]

$$r = \left\{ \sum_{i=1}^{R} i\,{}^{h}C_i K^i [\mathrm{S}]^i \right\} / \left\{ 1 + \Sigma\,{}^{h}C_i K^i [\mathrm{S}]^i \right\} \qquad (4a)$$

$${}^{h}C_i = \frac{(N - m(i-1) - n + i)!}{i!\,[N - m(i-1) - n]!} \qquad (4b)$$

As noted above, the correct quantitative interpretation of the equilibrium data is clearly predicated on the selection of the correct value of the thermodynamic capacity R, the determination of which requires experimental measurements that are likely to reflect the transient (pseudoequilibrium) state rather than thermodynamic equilibrium condition.

4. Discussion

The increasing availability of powerful computing facilities, in conjunction with developments in numerical algorithms, clearly offers the potential for more detailed probes into the kinetics of nonspecific binding of large ligands to sequences of identical (or extremely similar) residues on linear polymer lattices. This investigation follows on from the earlier findings of Epstein et al. [11–15], whose numerical simulation work had already established the possible existence of a biphasic time course for the attainment of equilibrium in the binding of ligands to nonspecific sequences of residues on a polymer lattice. The potential significance of those earlier observations is given greater focus by the present results, which serve to define more clearly the particular circumstances under which the consequences of the kinetics of elimination of the parking problem may pose difficulties for the collection of thermodynamic data on nonspecific ligand binding. From the present simulations it is evident that the potential for the existence of a transient plateau in the time course of equilibrium attainment increases dramatically with (i) increasing extent of acceptor saturation (see Fig. 5), (ii) increasing magnitude of the binding constant by virtue of the consequent decrease in k_r (Fig. 6), and (iii) increasing length of the linear acceptor—particularly in instances where the total number of lattice residues is a multiple of the number occupied by a ligand (Fig. 7). In an experimental situation it is therefore critical to check whether a seemingly stable response measured in (say) a spectrofluorometric study of nonspecific binding reflects the required thermodynamic equilibrium position or merely a

pseudoequilibrium position prior to elimination of the parking problem.

Simulations such as those presented here may, of course, overestimate the time required for equilibrium attainment because of their disregard of the potential consequences of restricted diffusion [21,22]. Indeed, those theoretical studies seem to have allayed concern about the need for checking whether experimental results obtained for all protein–polynucleotide and protein–polysaccharide interactions are in fact amenable to thermodynamic interpretation. What has been demonstrated is that a combination of extremely weak nonspecific binding and subsequent restricted diffusion of dissociated ligand along the chain can account for an abnormally high association rate constant such as that reported [23] but now refuted [24] for the specific interaction of *Escherichia coli* lac repressor with its operator. This sliding mechanism has also been proposed to account for the accelerated inhibition of thrombin by antithrombin III in the presence of heparin: nonspecific binding of the enzyme is considered to allow its diffusion in the dimension of the heparin chain towards the inhibitor bound to a specific pentasaccharidic sequence of the heparin [25]. Although such a mechanism may well apply to those particular situations involving weak nonspecific binding as an enhancer of the rate of specific binding that is governed by a much larger equilibrium constant, it does not signify a general irrelevance of the need to consider the consequences of the parking problem—particularly in instances where nonspecific interaction is the only binding event. Basically, any rearrangement of bound ligand molecules on an acceptor lattice must await dissociation of an unsaturable acceptor ligand complex (the cause of the parking problem); and although restricted diffusion can certainly increase the magnitude of the effective association rate constant, the rebinding of ligand is often effectively instantaneous on the time scale of ligand dissociation, which is the rate-limiting step.

The present illustration (Fig. 6) that attainment of a reasonable approximation to thermodynamic equilibrium in a reaction mixture may take several hours despite attainment of an essentially time-independent binding response within a matter of seconds is, of course, predicated by the use of relatively small magnitudes for k_r. Although it can be argued that such values are unreasonably small for some systems, and that equilibrium is likely to be attained much more quickly than is suggested by the illustration, the present findings may still retain relevance even under circumstances where equilibrium is attained within a few minutes. Whereas such a time requirement for attainment of equilibrium causes no concern whatsoever in a conventional spectrophotometric/spectrofluorometric titration, the need to monitor the binding response for that length of time in stopped-flow or temperature-jump studies of ligand binding is often not appreciated. In studies of nonspecific interactions between a large ligand and a polymeric acceptor lattice an experimenter may well be required to display considerable patience before interpreting a seemingly stable binding response as attainment of equilibrium, and hence as the parameter appropriate to analysis in terms of a thermodynamic binding expression.

Finally, it should be recalled that potential effects of the parking problem on the attainment of chemical equilibrium only represent a major source of concern for reaction mixtures in which there is a high extent of acceptor saturation; and that they do not pose a serious threat to the validity of the values of the equilibrium binding function, r_{eq}, in the range of acceptor saturation that is accessible to convenient measurement. The difficulty is encountered in the attempt to determine the maximal value or r, i.e., the acceptor capacity for ligand (R), knowledge of which is a prerequisite for establishing the appropriate binding equation for thermodynamic characterization of the interaction (Eqs. (4a) and (4b)). We have therefore employed results for the nonspecific interaction of thrombin with heparin [17] to explore the possibility of determining an acceptor capacity from stoichiometric titration curves, and then evaluating an equilibrium binding capacity on the basis that the determined value refers to the capacity under conditions where the parking problem is essentially irreversible (Table 2 and Fig. 8).

The scope of this investigation clearly needs to be extended to situations involving cooperative binding between ligand and nonspecific sequences of residues on a linear lattice—an endeavor for which an appropriate line of attack has again already been established [11,26]. However, although cooperative binding undoubtedly alters the quantitative manifesta-

tions of the kinetics of elimination of the parking problem, it is unlikely to affect the present qualitative conclusion that the current analysis of nonspecific binding to linear lattices needs closer scrutiny. We therefore hope that this study may stimulate further examination of the commonly held belief that the characterization of nonspecific binding to linear polymers only requires considerations of the thermodynamic manifestations of the parking problem.

Acknowledgements

The support of this investigation by the Australian Research Council is gratefully acknowledged.

References

[1] A.L. Latt, H.A. Sober, Biochemistry 6 (1967) 3293.
[2] J.D. McGhee, P.H. von Hippel, J. Mol. Biol. 86 (1974) 469.
[3] S.T. Olson, H.R. Halvorson, I. Björk, J. Biol. Chem. 266 (1991) 6342.
[4] R.C. Kelly, D.E. Jensen, P.H. von Hippel, J. Biol. Chem. 251 (1976) 7240.
[5] I.R. Epstein, Biophys. Chem. 8 (1978) 327.
[6] E. Di Cera, Y. Kong, Biophys. Chem. 61 (1996) 107.
[7] E. Di Cera, P.E. Phillipson, Biophys. Chem. 61 (1996) 125.
[8] T.L. Hill, Nature 274 (1978) 825.
[9] L.E. Greene, E. Eisenberg, J. Biol. Chem. 255 (1980) 549.
[10] I.R. Epstein, Biopolymers 18 (1979) 765.
[11] I.R. Epstein, Biopolymers 18 (1979) 2037.
[12] C. Dateo, I.R. Epstein, Biopolymers 20 (1981) 1651.
[13] J. Reiter, I.R. Epstein, J. Phys. Chem. 91 (1987) 4813.
[14] J. Reiter, I.R. Epstein, Biophys. Chem. 33 (1989) 1.
[15] J. Reiter, I.R. Epstein, Biopolymers 29 (1990) 543.
[16] P.J. Flory, J. Am. Chem. Soc. 61 (1939) 1518.
[17] M. Nesheim, M.N. Blackburn, C.M. Lawler, K.G. Mann, J. Biol. Chem. 261 (1989) 3214.
[18] Z.-R. Gan, Y. Li, Z. Chen, S.D. Lewis, J. Shafer, J. Biol. Chem. 269 (1994) 1301.
[19] W. Bode, R. Huber, T.J. Rydel, A. Tulinsky, (1992), in: L.J. Berliner (Ed.), Thrombin, Structure and Function, Plenum, New York, p. 3.
[20] B.N. Preston, J.M. Snowden, K.T. Houghton, Biopolymers 11 (1972) 1645.
[21] P.H. Richter, M. Eigen, Biophys. Chem. 2 (1974) 255.
[22] R. Schranner, P.H. Richter, Biophys. Chem. 8 (1978) 135.
[23] A.D. Riggs, S. Bourgeois, M. Cohn, J. Mol. Biol. 53 (1970) 401.
[24] R. Fickert, B. Müller-Hill, J. Mol. Biol. 226 (1992) 59.
[25] M. Hoylaerts, W.G. Owen, D. Collen, J. Biol. Chem. 259 (1984) 5670.
[26] E. Stutter, H. Stutz, Stud. Biophys. 66 (1977) 1.